New extended interpolating operators for hadron correlation functions

DIPARTIMENTO DI FISICA

SAPIENZA
UNIVERSITÀ DI ROMA

Mauro Papinutto

In collaboration with F. Scardino and S. Schaefer

based on Phys. Rev. D98 (2018) 094506

Excited QCD 2019, Schladming, 1st February 2019

Motivations

Two point hadron correlation functions in euclidean time are used to extract the spectrum:

$$\int d^3\mathbf{x}\langle B(\mathbf{x},t)\,\bar{B}(\mathbf{0},0)\rangle \quad \sim \quad \sum_n \langle 0|B|b_n\rangle\langle b_n|\bar{B}|0\rangle\, e^{-E_n t}$$

$$\overset{t\gg(E_1-E_0)^{-1}}{\longrightarrow} \quad \langle 0|B|b_0\rangle\langle b_0|\bar{B}|0\rangle\, e^{-E_0 t}$$

Exponential suppression of the signal-to-noise ratio in Euclidean time $\Rightarrow$ limits the attainable precision in lattice QCD computations of hadronic observables.

One first step, find improved interpolating operators which allow to decrease statistical and systematic errors in the extraction of the hadron spectrum, form factors and matrix elements (average moments of PDF, GPD, etc.):

- enhance the coupling to the ground state with respect to the excited states (essential because signal-to-noise ratio deteriorates with growing Euclidean time distances) allowing for plateau regions at earlier times;

- do not increase the statistical noise.

With respect to local (point) sources, the overlap with the ground state can be improved by using extended sources.

Smoothing techniques (smeared sources) based on the iterated application of the three-dimensional Laplace operator successful in many applications.

Drawback of smoothing techniques: quite empirical $\Rightarrow$ difficult to predict the relevant parameters as the lattice spacing is changed.

They provide a way to change the relative couplings of the various states which contribute to a given two-point function $\Rightarrow$ solve a generalized eigenvalue problem (GEVP) to get a better handle on the ground and excited states:

1. construct an Hermitian matrix of correlators from a basis of linearly independent operators:

$$C_{ij}(t) = \int d^3\mathbf{x} \, \langle O_i \bar{O}_j \rangle, \quad i, \, j = 1, \ldots, N.$$

2. solve the corresponding generalized eigenvalue problem

$$C(t) v_n = \lambda_n(t, t_0) C(t_0) v_n, \quad n = 1, \ldots, N.$$

3. the $\lambda_n(t, t_0)$ correspond then to the N energy states interpolated by the set of operators O_i via

$$E_n = \log \frac{\lambda_n(t,t_0)}{\lambda_n(t+a,t_0)} \qquad a = \text{lattice spacing.}$$

We propose here an alternative construction of extended interpolating operators based on (quenched) 3D fermions living on a single time-slice, which are suitably coupled to the physical quarks propagating in 4D.

Big advantage: this construction can be formulated in terms of a field theory $\Rightarrow$ theoretical control on renormalisation (i.e. approach to the continuum limit) $\Rightarrow$ show that short distance behaviour of two-point functions is greatly improved.

solution of a linear system to invert the 3D Dirac operator and obtain the 3D fermion propagator $\Rightarrow$ vast literature and improvements in this area can make it computationally economical.

3D fermions and extended operators

The 3D fermion fields φ are ordinary spin $1/2$ quark fields constrained to stay on the time-slice $x_0 = \tau$ with Lagrangian density:

$$\mathcal{L}_{3D} = \delta(x_0 - \tau) \sum_{i=1}^{N_f} \bar{\varphi}_i \left(\not{D} + m_{3D}^i \right) \varphi_i$$

In order for these objects not to propagate in time, we impose:

$$D_0 \varphi_i \big|_{x_0=\tau} = 0$$

and the action is

$$A_{3D} = \int d^3\mathbf{x} \sum_{i=1}^{N_f} \bar{\varphi}_i \left(\not{D} + m_{3D}^i \right) \varphi_i \qquad \text{with} \quad \not{D} = \gamma_k D_k.$$

The 3D fermions are quenched and therefore they only provide valence contributions.

However they are coupled to the spatial part of the gauge field and therefore receive quantum corrections and need to be renormalized.

We construct the extended quark operators by coupling the 3D fermions to the 4D quark fields ψ via bilinear operators:

$$q(\mathbf{x},t) = \int d^3\mathbf{y}\varphi(\mathbf{x})\ \bar{\varphi}(\mathbf{y})\gamma_5\psi(\mathbf{y},t)\ ,$$

The extended quark propagator, after integrating out both the 3D and 4D fermions, takes the form

$$\langle q(\mathbf{x}',t')\bar{q}(\mathbf{x},t)\rangle = \int d^3\mathbf{y}d^3\mathbf{y}' S_{3D}(\mathbf{x}',\mathbf{y}')\gamma_5 S_{4D}(\mathbf{y}',t',\mathbf{y},t)\gamma_5 S_{3D}(\mathbf{y},\mathbf{x})\ .$$

This construction immediately extends to meson and baryon operators. We call $\boldsymbol{B}$ the 3D baryon operator corresponding to a 4D baryon operator B (built by substituting the ψ with the φ) and we couple it with the appropriate number of

3D-4D bilinears in order to make it propagate through time

$$O_B(\mathbf{x},t) = \int d^3\mathbf{x_1} d^3\mathbf{x_2} d^3\mathbf{x_3}\, \boldsymbol{B}(\mathbf{x})\, \bar{\varphi}(\mathbf{x_1})\gamma_5\psi(\mathbf{x_1},t)\, \bar{\varphi}(\mathbf{x_2})\gamma_5\psi(\mathbf{x_2},t)\, \bar{\varphi}(\mathbf{x_3})\gamma_5\psi(\mathbf{x_3},t)$$

We immediately notice that while a normal baryon operator has canonical dimension $[B] = \frac{9}{2}$ the extended operator has a much lower one $[O_B] = \frac{3}{2}$.

The 3D fermions have an additional symmetry with respect to the 4D ones:

$$\varphi(\mathbf{x}) \to e^{i\alpha\Gamma}\varphi(\mathbf{x}), \qquad \bar{\varphi}(\mathbf{x}) \to \bar{\varphi}(\mathbf{x})e^{-i\alpha\Gamma}, \qquad U_i(x) \to U_i(x)$$

where $\Gamma = i\gamma_0\gamma_5$ is Hermitian and commutes with the 3D Dirac operator.

Using this symmetry together with Parity, Charge Conjugation and Cubic symmetry (on the lattice) it's easy to show that the action A_{3D} could mix only with $\bar{\varphi}\varphi$ and $\bar{\varphi}\not{D}\varphi$ which give the usual mass and field renormalisation.

Easy to show that the renormalisation constants Z_φ and δm_{3D} are $\log$ divergent at one loop like in the 4D case.

Using these symmetries also easy to show that the 3D baryon and meson operators as well as the 3D-4D bilinears are multiplicatively renormalisable.

When we combine these pieces together to create an extended interpolating operator, the worst divergence happens when all the bilinears get close to the 3D interpolating operator and OPE tells us that:

$$\boldsymbol{B}(0)\ \bar{\varphi}(\mathbf{x_1})\gamma_5\psi(\mathbf{x_1})\ \bar{\varphi}(\mathbf{x_2})\gamma_5\psi(\mathbf{x_2})\ \bar{\varphi}(\mathbf{x_3})\gamma_5\psi(\mathbf{x_3}) \to \frac{1}{(\mathbf{x}^2)^3}B(0) \quad \mathbf{x_1}, \mathbf{x_2}, \mathbf{x_3} \to 0$$

where $B(0)$ is the four dimensional baryonic operator.

Since there are three $3D$ integrations, the degree of divergence is $9 - 6 = 3 \Rightarrow$ the singularity is integrable and does not give rise to additional UV divergences.

$\Rightarrow$ The $3D$ extended operators are well behaved under renormalisation and are finite once the bilinears and interpolating operators are renormalized.

OPE and short distance behaviour

A standard baryon two-point function has dimension 9 $\Rightarrow$ at zero momentum, for small time t is badly divergent:

$$C_B(t) \sim \int d^3\mathbf{x}\, \frac{1}{(\mathbf{x}^2+t^2)^{9/2}} \sim \frac{64\pi}{105}\frac{1}{t^6}\ .$$

On the other hand, a baryon 3D extended operator has dimension $[O_B] = \frac{3}{2} \Rightarrow$ the corresponding two point function behaves much better at short times

$$C_{O_B}(t) \sim \int d^3\mathbf{x}\, \frac{1}{(\mathbf{x}^2+t^2)^{3/2}} \sim -8\pi \log\frac{t}{L}\ .$$

where we have considered a finite volume of linear size L with periodic boundary conditions.

The short distance behaviour is improved from a polynomial to a logarithmic divergence.

For the mesons, a local interpolating operator has dimension 3 and therefore its two point function at small time t diverges as

$$C_M(t) \sim \int d^3\mathbf{x} \, \frac{1}{(\mathbf{x}^2+t^2)^3} \sim \frac{\pi^2}{2t^3}$$

On the other hand a 3D extended meson operator has dimension 1 and its corresponding two point function has small t divergences at all

$$C_{O_M}(t) \sim \int d^3\mathbf{x} \, \frac{1}{\mathbf{x}^2+t^2} \sim 4\pi L$$

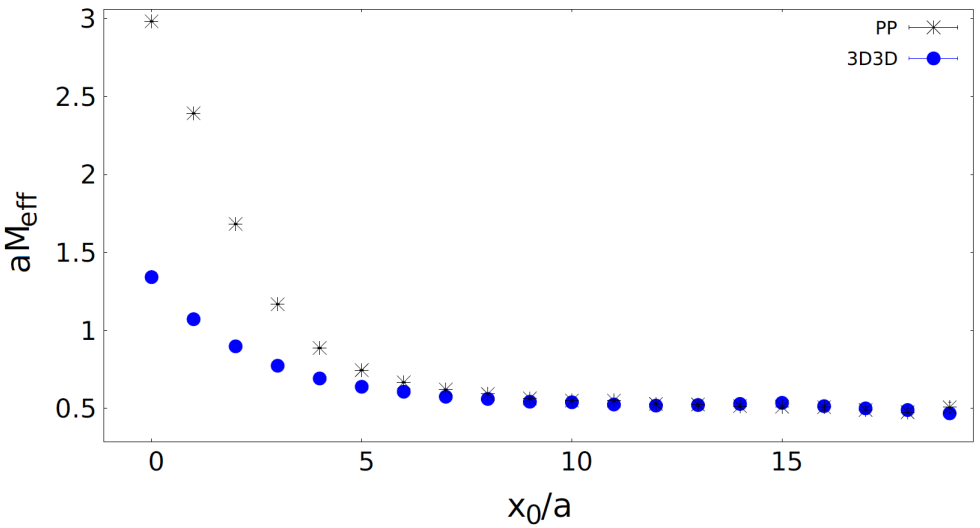

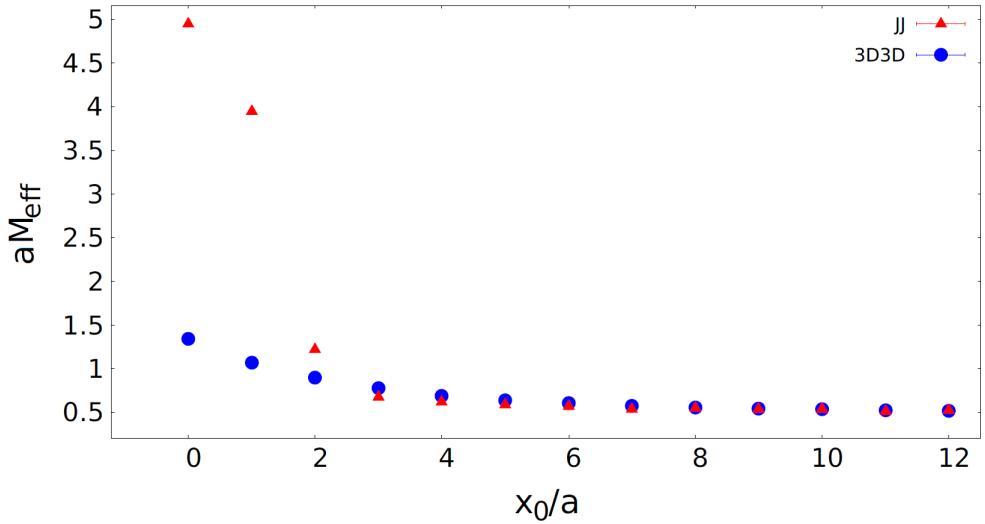

Numerical results

Lattice QCD simulations performed on the CLS $N_f = 2 + 1$ gauge configurations. In the present exploratory study we have used the flavour $SU(3)$ symmetric 96×32^3 ensemble with $M_\pi = M_K = 420\,\text{MeV}$ and a lattice spacing $a = 0.086\,\text{fm}$

We have measured two matrices of correlators by using a basis of 3 Nucleon and 2 Ω interpolating operators belonging to different representation of the cubic group.

We plot below the shape of the modulus squared of the 3D propagator $|\psi|^2 = |S_{3D}(0, r)|^2$, where S_{3D} appears in the extended operators, at different values of m_{3D}. The lighter the 3D fermions are, the more the sources are extended in space.

The modulus squared of the $3D$ propagator can be interpreted as the propagator of a pion, that propagates in two spatial dimensions plus a fictitious temporal direction which coincides with the third spatial direction on a fixed time-slice $\Rightarrow$ the width of the sources can be linked to the mass of such 3D pion.

The mass the 3D pion M_π^{3D} can thus be measured and it turns out that its square depends linearly on the the 3D quark mass m_{3D} as in 4D.

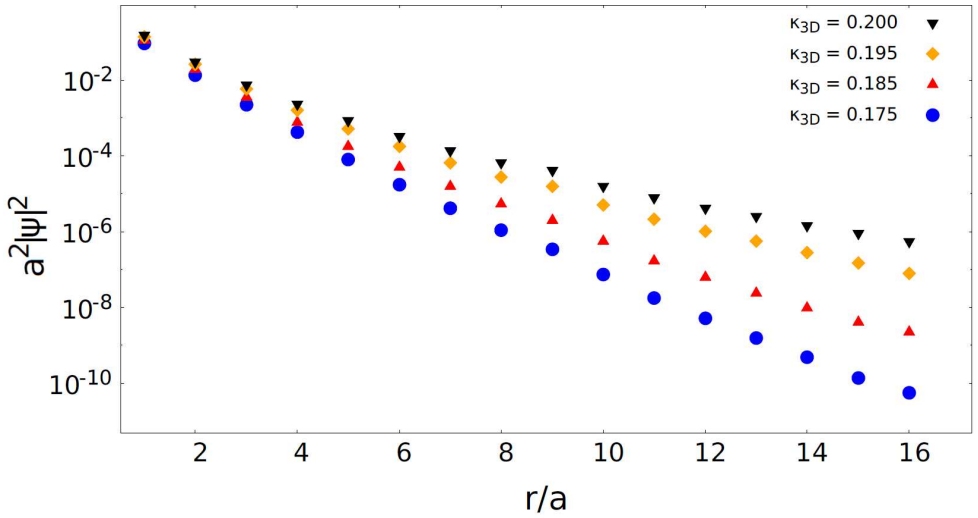

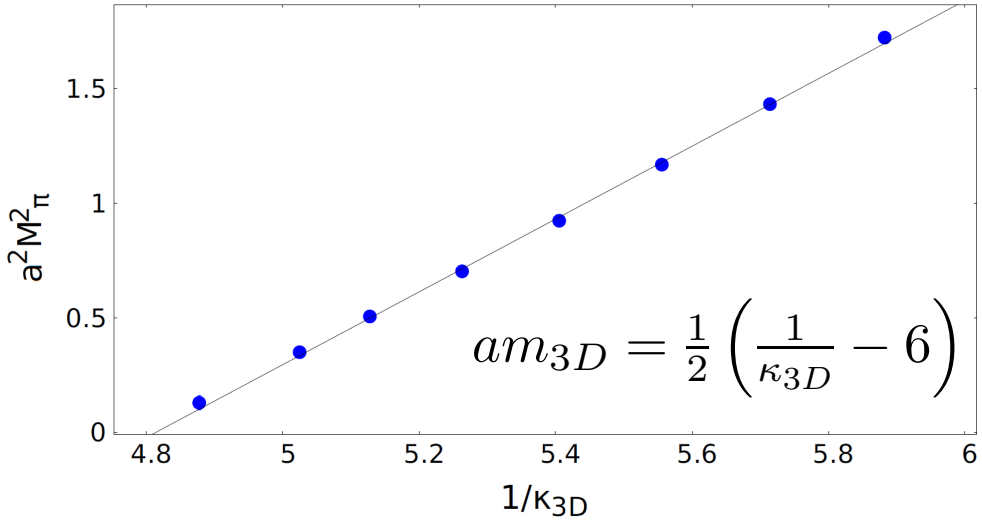

The size of the 3D extended operators is thus controlled by the 3D pion mass, which do not renormalise in the continuum limit. It is thus very easy to control their size when varying the lattice spacing.

The mass of the 3D fermion affects the shape of the 3D extended operator and must also change how it couples to different states. We have thus computed the effective mass of the Nucleon and fitted it to the form

$$M_{eff}(t) = M + re^{-(E-M)t}$$

where we have modelled the coupling to the excited states in a single term with a parameter r which regulates the strength of the coupling.

r plotted as a function of κ_{3D} shows that the coupling to the excited states changes rather dramatically by changing κ_{3D}. The more extended the operators are, the less they couple to the excited states.

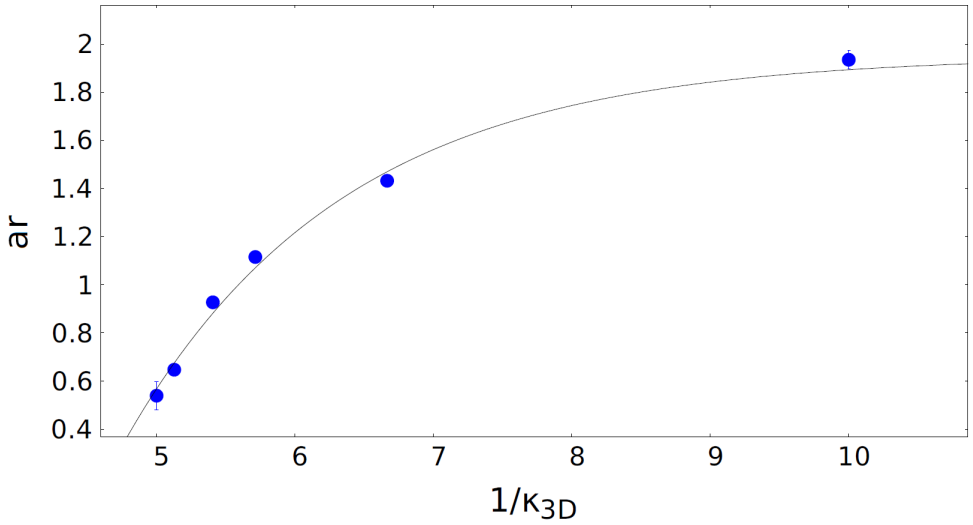

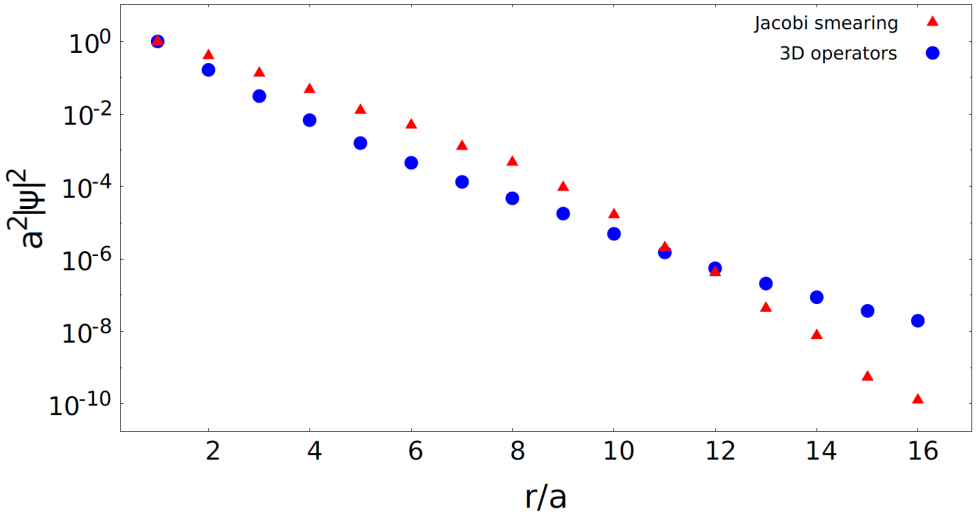

To compare the effectiveness of the 3D extended operator technique relative to the existing ones, we have computed the baryonic two point functions with standard local sources and Jacobi smeared sources.

Free parameters of the Jacobi smearing are the number of terms included into the sum N_{sm} and κ_{sm} which regulates how strongly the source is spread out:

$$\Psi_{\mathrm{sm}} = \sum_{n=0}^{N_{sm}} (\kappa_{sm}\Delta)^n \, \delta(\mathbf{x})$$

The parameters have been chosen to be $N_{sm} = 50$ and $\kappa_{sm} = 0.20$, such that the square of the source radius matches to the one of the 3D fermions (for which $\kappa_{3D} = 0.185$).

The Jacobi smeared source Ψ_{sm} behaves very differently from the 3D one. The latter has the typical exponential decay in the long distance region, whereas the Jacobi source has a shape similar to a Gaussian.

The different shapes of these two source types give the opportunity to construct operators that differ significantly from one another and solve the GEVP.

The two point functions obtained from the Jacobi and local sources have a very singular behaviour at short distances while the 3D operators are much better behaved.

Furthermore we can clearly infer from a zoom onto the plateau region that Jacobi-Jacobi correlators are noisier than 3D-3D extended operators ones even though the plateau region starts at comparable times.

The effective masses $M_{eff}(x_0)$ have been fitted with the same function we have defined before, in the range $[t, t_{max}]$, allowing us to study the stability of M and r with the different methods when they are studied as functions of t.

The comparison between the different methods also requires a discussion of their computational cost. At our simulation parameters, Jacobi smearing and 3D operators take roughly the same computer time.

$\Rightarrow$ Constructing the source takes roughly 5% of the time to invert the 4D Dirac operator. Even the 3D inversion for the sink (on all time slices) can be done in a fifth of the time of the latter.

The 4D operator is inverted using an advanced technique called deflation. 5while the 3D inversions with a simple conjugate gradient algorithm. In case of even wider sources, or many smoothing radii, deflation techniques could certainly be used to significantly speed up the 3D inversions.

Op.	ar	am	aE_1	t/a
$3D_1$	0.820 $\pm$ 0.003	0.519 $\pm$ 0.0024	0.907 $\pm$ 0.006	1
$3D_1$	0.811 $\pm$ 0.007	0.517 $\pm$ 0.0027	0.898 $\pm$ 0.009	2
$3D_1$	0.811 $\pm$ 0.017	0.517 $\pm$ 0.0032	0.898 $\pm$ 0.013	3
$3D_1$	0.767 $\pm$ 0.033	0.518 $\pm$ 0.0037	0.878 $\pm$ 0.019	4
$3D_1$	0.692 $\pm$ 0.057	0.512 $\pm$ 0.0044	0.849 $\pm$ 0.027	5
$3D_1$	0.733 $\pm$ 0.127	0.513 $\pm$ 0.0051	0.863 $\pm$ 0.042	6
$3D_1$	0.808 $\pm$ 0.281	0.514 $\pm$ 0.0059	0.880 $\pm$ 0.069	7
$3D_1$	0.504 $\pm$ 0.307	0.509 $\pm$ 0.0093	0.805 $\pm$ 0.109	8
$3D_1$	0.640 $\pm$ 0.807	0.511 $\pm$ 0.0106	0.839 $\pm$ 0.186	9

Op.	ar	am	aE_1	t/a
J_1	4.828 $\pm$ 0.329	0.456 $\pm$ 0.0959	1.159 $\pm$ 0.169	1
J_1	16.981$\pm$ 0.685	0.548 $\pm$ 0.0074	2.157 $\pm$ 0.042	2
J_1	11.871$\pm$ 3.386	0.544 $\pm$ 0.0081	1.981 $\pm$ 0.143	3
J_1	0.479 $\pm$ 0.068	0.512 $\pm$ 0.0063	0.877 $\pm$ 0.052	4
J_1	0.384 $\pm$ 0.093	0.508 $\pm$ 0.0086	0.819 $\pm$ 0.075	5
J_1	0.357 $\pm$ 0.161	0.506 $\pm$ 0.0110	0.803 $\pm$ 0.113	6
J_1	0.213 $\pm$ 0.125	0.497 $\pm$ 0.0238	0.692 $\pm$ 0.163	7
J_1	0.382 $\pm$ 2.062	0.194 $\pm$ 2.106	0.208 $\pm$ 2.201	8

The single 3D operator is very stable when starting the fit at very short distances and remains stable starting fit at larger times (up to $t = 9$).

The fit of a single Jacobi operator is unstable at short distances and converges very slowly at larger times where the signal begins to fade into noise much faster than in the 3D case (for $t = 8$ the signal is already lost).

We have then proceeded by solving the GEVP with a basis of two operators.

Basis	ar	am	aE_1	t/a
$\{3D_0, 3D_1\}$	0.818 ± 0.003	0.521 ± 0.0025	0.912 ± 0.006	1
$\{3D_0, 3D_1\}$	0.813 ± 0.006	0.519 ± 0.0028	0.906 ± 0.008	2
$\{3D_0, 3D_1\}$	0.820 ± 0.016	0.520 ± 0.0033	0.910 ± 0.013	3
$\{3D_0, 3D_1\}$	0.776 ± 0.034	0.518 ± 0.0038	0.891 ± 0.019	4
$\{3D_0, 3D_1\}$	0.726 ± 0.065	0.516 ± 0.0046	0.873 ± 0.028	5
$\{3D_0, 3D_1\}$	0.841 ± 0.158	0.518 ± 0.0050	0.905 ± 0.045	6
$\{3D_0, 3D_1\}$	1.168 ± 0.489	0.521 ± 0.0050	0.961 ± 0.078	7
$\{3D_0, 3D_1\}$	0.876 ± 0.745	0.519 ± 0.0068	0.918 ± 0.137	8
$\{3D_0, 3D_1\}$	0.388 ± 0.586	0.515 ± 0.0131	0.804 ± 0.231	9

Basis	ar	am	aE_1	t/a
$\{J_0, J_1\}$	4.843 ± 0.339	0.457 ± 0.0932	1.164 ± 0.166	1
$\{J_0, J_1\}$	17.469 ± 0.662	0.540 ± 0.0065	2.162 ± 0.039	2
$\{J_0, J_1\}$	17.127 ± 5.512	0.539 ± 0.0072	2.152 ± 0.161	3
$\{J_0, J_1\}$	0.403 ± 0.068	0.511 ± 0.0066	0.865 ± 0.061	4
$\{J_0, J_1\}$	0.298 ± 0.080	0.505 ± 0.0097	0.786 ± 0.084	5
$\{J_0, J_1\}$	0.274 ± 0.131	0.503 ± 0.0127	0.766 ± 0.124	6
$\{J_0, J_1\}$	0.157 ± 0.057	0.485 ± 0.0424	0.619 ± 0.180	7
$\{J_0, J_1\}$	0.428 ± 2.898	0.141 ± 2.942	0.151 ± 3.032	8

Basis	ar	am	aE_1	t/a
$\{P_0, P_1\}$	2.628 $\pm$ 0.060	0.459 $\pm$ 0.0445	0.874 $\pm$ 0.068	1
$\{P_0, P_1\}$	3.366 $\pm$ 0.047	0.532 $\pm$ 0.0081	1.102 $\pm$ 0.018	2
$\{P_0, P_1\}$	3.877 $\pm$ 0.138	0.544 $\pm$ 0.0060	1.167 $\pm$ 0.020	3
$\{P_0, P_1\}$	3.141 $\pm$ 0.219	0.535 $\pm$ 0.0058	1.097 $\pm$ 0.026	4
$\{P_0, P_1\}$	2.104 $\pm$ 0.177	0.523 $\pm$ 0.0048	0.989 $\pm$ 0.026	5
$\{P_0, P_1\}$	1.381 $\pm$ 0.159	0.514 $\pm$ 0.0049	0.896 $\pm$ 0.029	6
$\{P_0, P_1\}$	0.980 $\pm$ 0.183	0.507 $\pm$ 0.0065	0.830 $\pm$ 0.041	7
$\{P_0, P_1\}$	0.647 $\pm$ 0.188	0.498 $\pm$ 0.0103	0.755 $\pm$ 0.061	8
$\{P_0, P_1\}$	0.365 $\pm$ 0.122	0.478 $\pm$ 0.0257	0.640 $\pm$ 0.095	9

Results for the 3D extended operators are stable for any value of t_0, having very small short distance divergences. On the other hand the Jacobi and local sources need a larger t_0 to be away from the divergent short distance behaviour, in the analysis we have found that $t_0 = 4a$ allows for a fair comparison between the methods.

For the 3D basis, the GEVP doens't improve the results obtained with a single operator, which are already very stable. For the Jacobi smeared sources GEVP shows a modest improvement but results remain quite unstable.

Conclusions and outlook

- Quenched 3D fermions allow for a formulation of the extended operators in terms of a renormalizable field theory. The only free parameter is the mass of the 3D fermions which is easily adjustable through its connection with the pseudoscalar meson mass.

- 3D extended operators improve the short distance behaviour of the two point functions and that they are well behaved under renormalization so that the continuum limit can be taken in a controlled way.

- The disappearance of short distance divergences might improve the study of excited states, where a strong signal is needed at short Euclidean times.

- 3D extended operators are as computationally efficient as the Jacobi smearing for a large range of 3D masses even without optimisations for the evaluation of the 3D propagators.

- Numerical simulations of the two point functions of the nucleon and the Omega show that 3D extended operators can be used to obtain very precise results.

- The differences in the short distance behaviour with respect to Jacobi smearing make the 3D extended operators a very interesting complement to the basis used in the GEVP $\Rightarrow$ they look promising in increasing the precision in the extraction of hadron quantities.